Computers in Biology and Medicine 196 (2025) 110686

Contents lists available at ScienceDirect

Computers in Biology and Medicine

journal homepage: www.elsevier.com/locate/compbiomed

Influence of pre-bending on primary fixation stability in one-segmental mandibular reconstruction

Philipp Ruf [a,b], Özgür Cebeci [b], Vincenzo Orassi [b], Claudius Steffen [a], Georg N. Duda [b], Max Heiland [a], Sara Checa [b,c,*,1], Carsten Rendenbach [a,1]

[a] Department of Oral and Maxillofacial Surgery, Charité – Universitätsmedizin Berlin, Corporate member of Freie Universität Berlin and Humboldt-Universität zu Berlin, Augustenburger Platz 1, 13353, Berlin, Germany
[b] Julius Wolff Institute, Berlin Institute of Health at Charité - Universitätsmedizin Berlin, Augustenburger Platz 1, 13353, Berlin, Germany
[c] Institute of Biomechanics, Hamburg University of Technology (TUHH), Denickestrasse 15, 21073, Hamburg, Germany

ARTICLE INFO

Keywords:
Mandibular reconstruction
Finite element analysis
Conventional reconstruction plate
Patient-specific reconstruction plate
Biomechanics
Pre-bending
Stress
Strain

1 ABSTRACT

Background: The fixation of osseous free flaps for segmental mandible reconstruction after resection is most commonly performed with patient-specific 3D printed or conventional load-bearing reconstruction plates. The main challenge with conventional plates is the step of manual bending to adjust the plate to the specific mandible of the patient. To date, the influence of this permanent plate deformation on the biomechanical conditions within the healing regions remains unknown.
The present study aimed to investigate the effect of plate pre-bending on intersegmental strains, known to influence the healing outcome.
Methods: To achieve this, biomechanical finite element models were developed to simulate plate pre-bending and biting in a one-segmental mandibular reconstruction. The biomechanics induced within the healing region were compared between a pre-stressed conventional reconstruction plate and a customized conventional reconstruction plate.
Results: Higher stresses were predicted in the pre-stressed plate. However, the mechanical strains within the healing regions were not influenced by plate pre-bending.
Conclusions: The increased levels of mechanical strains under both pre-stressed and customized conventional plates in comparison to common patient-specific plates could be a reason for the higher rates of osseous union under conventional fixation. Since customized conventional reconstruction plates additionally presented elastic stresses and include the advantages of patient-specific plates, those plates are biomechanically and clinically promising.

1. Introduction

Due to high rates of osseous non-union, mandibular reconstruction after segmental resection with the gold standard fibula free flap remains a clinical challenge [1,2]. Although patient-specific reconstruction plates have demonstrated clinical advantages such as reduced surgery time (patient-specific: 213 min–575 min; conventional: 211 min–738 min [3]) and increased precision, significantly higher rates of osseous union have been reported for conventional reconstruction plates [2,4,5]. Knitschke et al. reported long-term non-union rates at least 36 months after surgery of 4.2 % for conventional plates and 18.2 % for patient-specific plates [6]. Previous studies have suspected mechanical factors as causal for this observation [2,4,7,8]. Other advantages of conventional plates are lower production costs and a shorter time from diagnosis to therapy because the production process of patient-specific 3D-printed reconstruction plates is avoided [5].

The key difference between custom and conventional plates is the pre- or intraoperative pre-bending step necessary for conventional plates [7,9–11]. This requires a different plate design in conventional plate systems, with a slim shape between screw holes and the use of pure titanium [4,7,12,13]. Pure titanium has the advantage of a broad plastic phase, which allows for permanent plastic deformation [14]. In contrast,

* Corresponding author. Augustenburger Platz 1, 13353, Berlin, Germany.
E-mail address: sara.checa@charite.de (S. Checa).
[1] These authors contributed equally to this work (co-last/equal authorship).

https://doi.org/10.1016/j.compbiomed.2025.110686
Received 18 November 2024; Received in revised form 6 April 2025; Accepted 26 June 2025
Available online 3 July 2025

patient-specific plates use the titanium alloy Ti6AlV4 with a high yield strength but a narrow plastic phase [15–17]. A previous study demonstrated plastic stresses in conventional plates due to pre-bending [10]; however, the impact of plate pre-bending on the biomechanical conditions within the bone healing region was not evaluated. These conditions are particularly relevant since in the initial healing phase, intersegmental strains have been described as the main mechanical stimulus determining the bone regeneration outcome [18–21].

Therefore, the present study aimed to evaluate the influence of plate pre-bending on the intersegmental strains in the healing regions.

2. Materials and methods

A finite element (FE) model representing the pre-bending of a commercially available conventional reconstruction plate was established on a mandible reconstruction with a one-segmental fibula free flap. In a second step, the fixed reconstructed mandible was investigated under fixation with both the pre-bent reconstruction plate and a same-shaped customized reconstruction plate. Screw fixation did not differ between the two models. The mechanical stresses in the plates and the strains in the healing regions were evaluated.

2.1. Reconstructed mandible model geometry

The primary model geometry was initially developed for a previous study [16] and has been modified to address the research question of the present study. This geometry was derived from a pre-operative axial computer tomography (CT) scan of a 57-year-old female patient undergoing segmental mandibular resection due to oral squamous cell carcinoma with bone invasion. Image segmentation and meshing were conducted using Amira 6.0.1 (Thermo Fisher Scientific, Waltham, Massachusetts, United States), by virtually distinguishing the mandible and right fibula into cortical and trabecular bone based on their gray-scale values. The cortical bone was identified for Hounsfield Units ranging from 300 to 2200 on the mandible and 250–2200 on the fibula, while the remaining inner bone areas were categorized as trabecular bone and medullary space.

Using the 3D computer-aided design (CAD) software SolidWorks 2020 (Dassault Systèmes, Vélizy-Villacoublay, France), the mandible was virtually resected and the fibula segment was placed from the right mandibular angle to the right canine region, using an extruded trapezoidal geometry as a resection guide. The fibula segment measured 5 cm in length and had a maximum diameter of 1.2 cm. It was positioned according to current surgical guidelines [22], leaving an 8 cm residual stump.

In the finite element analysis software Abaqus CAE 2021 (Dassault Systèmes, Vélizy-Villacoublay, France), the residual mandible cortical and trabecular geometries, along with the complementary fibula cortical and medullary space geometries, were merged into one volume part with four subdivided geometry sets. Intersegmental gaps were defined by creating a joint volume of the mandible and fibula at the interosseous interface with a width of 1 mm, as recent findings show that excessive gap width negatively impacts bone healing outcomes [23,24]. These intersegmental gaps represented the regions of interest (ROIs) where mechanical strains were evaluated.

2.2. Meshing and mesh convergence study

In line with previous FE studies of the mandible, the mandible and the screws were meshed in Abaqus CAE 2021 using second-order quadratic tetrahedral elements (Type C3D10) [16,25–27]. This mesh was based on the primary mesh assigned to the geometries in the segmentation software Amira 6.0.1. The mesh convergence test for the healing regions, performed in a previous study, was considered valid for this study since no changes were made to the underlying geometries [16]. Based on this mesh convergence analysis, an element size of 0.2 mm was chosen for the healing regions. The mesh size for the screws was set to 1.0 mm.

To enable the multi-step analysis, the reconstruction plate was meshed with quadratic hexahedral elements (type C3D20R). For the pre-bending of the reconstruction plate, a mesh convergence test was conducted. Mesh sizes of 0.5 mm, 0.4 mm, 0.3 mm, and 0.25 mm were tested. Transverse bending in both directions was separately investigated, both with 10° and 45°. The investigated output parameters were plastic equivalent strain, maximum plastic strain (absolute), and von Mises stresses. For the plate, the relative difference to the next finer mesh was below 5 % for all investigated parameters and scenarios for the 0.3 mm mesh. Consequently, a mesh size of 0.3 mm for the reconstruction plate was chosen.

2.3. Conventional plate assessment including pre-stress

To evaluate the effect of pre-bending on the mechanical conditions within the healing region, the reconstruction plate was assessed with and without pre-stress. A commercially available reconstruction plate (Karl Leibinger Medizintechnik GmbH & Co. KG, Tuttlingen, Germany) made of pure titanium with a thickness of 2.0 mm and locking threads (article number 50-775-26-XX) was chosen [12]. The STL files of the reconstruction plate in both non-bent and pre-bent conditions (including required bending angles) were received from the manufacturer.

For the fixation of the reconstruction plate, 7 mm monocortical screws were used on the fibula to prevent damage to the intraosseous vessels [12,22]. On the mandible, bicortical screws of varying lengths were used, as reported in previous studies [11,16,17]. The screw lengths are detailed in Fig. 1.

Since individual meshing of the plates with hexahedral elements is required for the multi-step analysis, the unbent plate was reconstructed as volume part in SolidWorks 2020. The simulation of pre-bending was performed in Abaqus CAE 2021. The undeformed reconstruction plate was bent to the specified shape. Therefore, kinematic coupling constraints between the midpoints of the anterior and posterior cross-section and the corresponding cross-section planes were employed. The bending was simulated in local coordinate systems for each bending area by defining a rotation of the anterior cross-section plane around the anterior midpoint, while the posterior plane was fixed (Fig. 1). Following the initial deformation, the plate was released to allow a “spring-back” and obtain the permanently deformed shape of the pre-stressed plate defined by the final bending angles specified in Fig. 1. Thereafter, the pre-stressed plate was re-imported for the biting analysis using the predefined field initial state option in Abaqus CAE 2021 [28]. Additionally, the biting simulation was conducted also with the customized plate (import of the deformed plate without pre-stress) for the sake of comparison. Table 1 presents all different plate types discussed within the present study.

2.4. Constraints, loading, and boundary conditions in the biting simulation

For both fixation scenarios, tie constraints were defined between the screws and plates as well as between the screws and the underlying bone tissue. This represents the simulation of locking screws, which are commonly used in fibula free flap surgery [29,30].

Two different biting tasks were investigated: incisal biting and unilateral biting. To simulate unilateral biting, the premolars and the first molar were restricted from vertical displacement. For incisal biting, the incisors were restricted from vertical movement. The condyles were

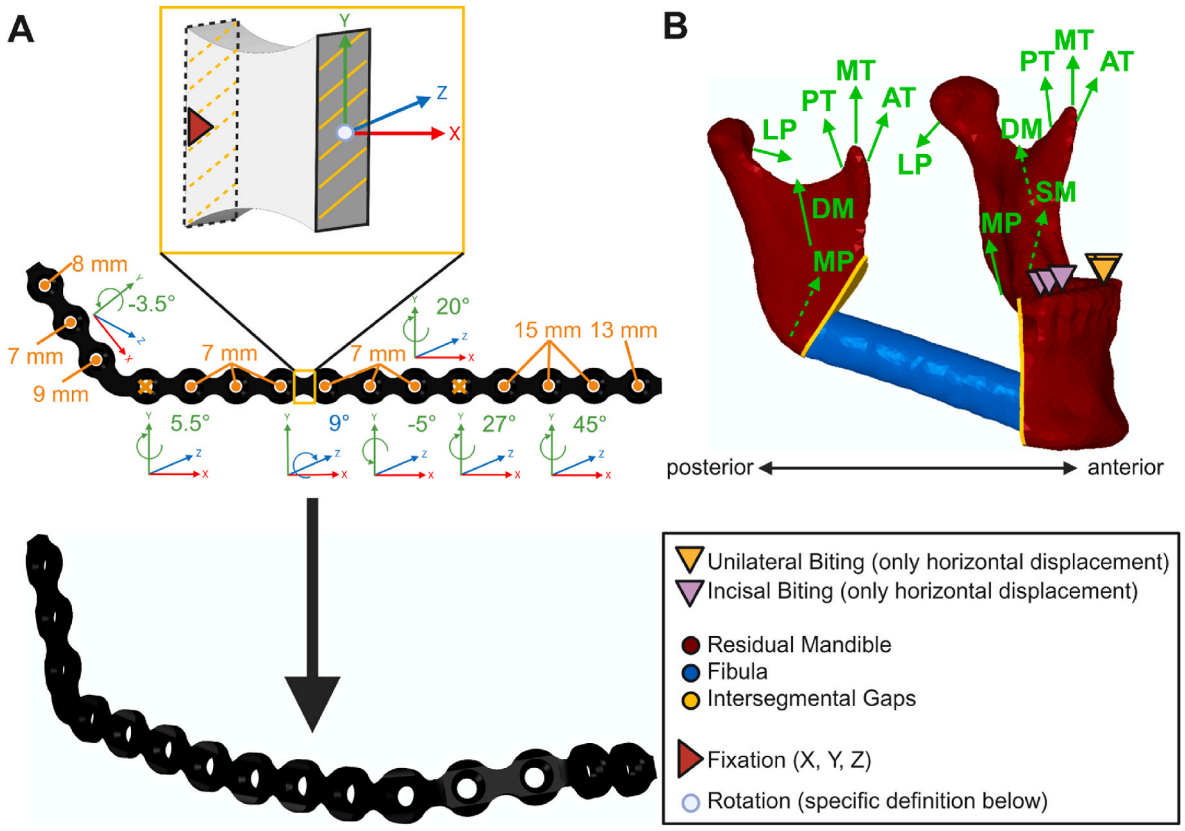

Fig. 1. (A) Reconstruction plate in undeformed and pre-bent configuration; bending angles (coordinate systems) and screw lengths (in orange) for reconstruction plate fixation; graphic description of the constraints within one exemplary bending segment: fixed posterior midpoint and its coupled cross-section along with the anterior midpoint and the coupled cross-section where rotation and deformation were defined; (B) overview over biting muscles of the reconstructed mandible including superficial- (SM) and deep masseter (DM), lateral- (LP) and medial pterygoid (MP) and anterior- (AT), middle- (MT) and posterior temporalis (PT) under unilateral and incisal biting (both boundary condition areas marked with multiple triangles) - Created with BioRender.com. (For interpretation of the references to colour in this figure legend, the reader is referred to the Web version of this article.)

assumed locked in the glenoid fossa, preventing movement in all degrees of freedom.

The main biting muscles involved were defined as loads, including the superficial- and deep masseter, anterior-, middle-, and posterior temporalis, and medial- and lateral pterygoid (Fig. 1). To simulate a post-operative scenario, maximum muscle forces and fiber activations from previous studies investigating the healthy mandible were adapted [31,32]. On the resection side (right), the superficial masseter was assumed to be detached, and the deep masseter was simulated as partially detached (50 % reduced fiber activation) [16]. The maximum muscle forces were assumed to be reduced to 12.5 %, resulting in a biting force of 40 N under unilateral biting, which is consistent with reported post-surgery values [33]. Maximum muscle forces, fiber directions and fiber activations are detailed in Table 2. Muscle insertion areas are presented in Fig. 1.

2.5. Material properties

Anisotropic, homogeneous, linear elastic material properties were assigned to the cortical bony structures using local coordinate systems [16,17,34–37]. On the mandible, the different cortical regions were assigned individual local coordinate systems where the principal axis was selected to be aligned with the main bony fiber direction of that specific region according to Schwartz-Dabney and Dechow [34]. Isotropic, homogeneous, linear elastic material properties were assigned to mandible trabecular bone, dentine, granulation tissue, and the screws [15–17,31,38,39] (Table 3). Granulation tissue was assumed both in the interosseous gap and the fibula medullary area. Below the yield stress, linear elastic material properties were assigned to the reconstruction plate (Table 3). The screws were assumed made of titanium alloy Ti6Al4V, whereas the reconstruction plate was considered made of pure titanium [12,14,15].

To model isotropic homogeneous linear plastic deformation beyond the nominal yield stress (340 MPa) in Abaqus CAE 2021, the software uses true stress (σ^t) and true strain (ε^t) [28]. These are calculated from nominal stress (σ^{nom}) and nominal strain (ε^{nom}) using the following formulas:

$$\varepsilon^t = \ln(1+\varepsilon^{nom})$$

$$\sigma^t = \sigma^{nom}(1+\varepsilon^{nom})$$

Based on true stress and true strain, the plastic strain (ε^{pl}) is calculated using the Young's modulus (E, 102 GPa [14]) with the formula:

$$\varepsilon^{pl} = \varepsilon^t - \frac{\sigma^t}{E}$$

Table 1
Plate types discussed in the present study along with their characteristics, materials, and usage.

Plate type	Characteristics	Material	Usage
Conventional reconstruction plate	• pre- or intraoperative pre-bending for the plate to fit the patient's anatomy [5] • slim bridges between the screw holes are required to enable pre-bending [4] • cheap and easy to access since no pre-planning is required [5]	• pure titanium [12]	• gold standard for mandibular reconstruction [5]
Common patient-specific reconstruction plate	• pre-planned reconstruction plate fits the patient's anatomy • reduced surgery time and increased precision [3] • often designed without slim bridges since no pre-bending is required ("reconstruction bar") [4] • induces higher rates of osseous non-union compared to conventional reconstruction plate [2,4,6]	• titanium alloy Ti6Al4V [16]	• trend towards patient-specific plates has been reported [5]
Customized conventional reconstruction plate	• theoretical concept plate used as control scenario in the present study • exactly same shape as conventional reconstruction plate → imported to the analysis without pre-stress values • from a mechanical perspective a patient-specific plate • could be manufactured analogously to common patient-specific plates using selective laser-melting [29]	• pure titanium	• not used for mandibular reconstruction

From the available data for pure titanium, the ultimate stress (430 MPa) was used as the top value for nominal stress, and elongation at break (28 %) was used as the top value for nominal strain [14]. Between the yield stress and the ultimate stress, the values were interpolated to obtain a curve of true stress and true strain which is detailed in Fig. 2.

2.6. Output evaluation

Mechanical strains within the healing regions were evaluated as indicators of the expected healing outcome. For the straining evaluation, only elements with absolute strains higher than 500 μstrain were included to minimize the influence of elements with small strain levels that are not part of the direct interosseous interface of different-sized mandible and fibula. Before strain data visualization, outlier values were identified using the ROUT method (combination of robust regression and outlier removal) with Q = 0.1 % [40] and removed for visualization.

Peaks in von Mises stress in the plates were calculated as an indicator of material failure. To achieve this, the average of the stresses in the 10 elements with the highest values in the percentile group [0 %; 99.97 %] was calculated. The largest 0.03 % of all stress values were excluded to minimize the effect of stress singularities that could occur due to tie constraints between objects with different mesh sizes and the kinematic coupling constraints in the plate bending [16,26].

Analogously to previous studies, all values were collected from the integration point of each element [16,26].

3. Results

The bite force in the different plating scenarios was predicted to be between 37 and 40 N for unilateral biting and between 9 and 10 N for incisal biting.

3.1. Intersegmental strains do not differ between pre-stressed plate and customized plate

The strain distributions under unilateral biting are shown in Fig. 3. Similar strain levels were observed in the intersegmental gaps with and without plate pre-stress in the posterior region (customized conventional reconstruction plate percentiles 1–4 %, 0.75–1.3 %, 0.5–0.8 %, 0.25–0.4 %; pre-bent conventional reconstruction plate percentiles 1–4 %, 0.75–1.3 %, 0.5–0.8 %, 0.25–0.4 %). Posterior strains were higher than anterior strains for both reconstruction plates with and without pre-stress (anterior customized conventional reconstruction plate percentiles 1–1.1 %, 0.75–0.4 %, 0.5–0.3 %, 0.25–0.2 %; anterior pre-bent conventional reconstruction plate percentiles 1–1.1 %, 0.75–0.4 %, 0.5–0.3 %, 0.25–0.2 %).

Table 2
Healthy maximum muscle forces, reduced maximum muscle forces on 12.5 %, fiber directions and fiber activations for the participating muscles in the investigated biting tasks unilateral (UNI) and incisal (INC) biting; fiber direction definition relative to the frontal (XY), transversal (XZ), and sagittal (YZ) planes [32].

	Healthy Maximum Muscle Force (N)	12,5 % of Maximum Muscle Force (N)	Fiber direction				Fiber activation			
			X		Y	Z	INC		UNI	
			Right	Left			Right	Left	Right	Left
Superficial Masseter	190,4	23,8	−0,207	0,207	0,884	0,419	0	0,4	0	0,72
Deep Masseter	81,6	10,2	−0,546	0,546	0,758	−0,358	0,13	0,26	0,3	0,72
Medial Pterygoid	174,8	21,85	0,486	−0,486	0,791	0,373	0,78	0,78	0,6	0,84
Lateral Pterygoid	66,9	8,3625	0,63	−0,63	−0,174	0,757	0,71	0,71	0,65	0,3
Anterior Temporalis	158	19,75	−0,149	0,149	0,988	0,044	0,08	0,08	0,58	0,73
Middle Temporalis	95,6	11,95	−0,222	0,222	0,837	−0,5	0,06	0,06	0,67	0,66
Posterior Temporalis	75,6	9,45	−0,208	0,208	0,474	−0,855	0,04	0,04	0,39	0,59

Table 3
Anisotropic and isotropic material properties for bone, intersegmental gaps, and fixation materials. 1: longitudinal (local bone orientation); 2: tangential; 3: transverse.

Material	Symphysis	Body	Angle	Ramus	Condyle	Coronoid	Fibula cortical	Dentin	Mandible trabecular	Granulation Tissue	Ti-6AI-4V	Titanium
E1 (GPa)	20,5	21,7	23,8	24,6	23,5	28	28	17,6	0,3	0,001	114	102
E2 (GPa)	16,4	17,8	19	18,4	17,9	17,5	17,7	17,6	0,3	0,001	114	102
E3 (GPa)	12,1	12,7	12,8	13	12,7	14	17,7	17,6	0,3	0,001	114	102
Nu12	0,34	0,34	0,3	0,28	0,24	0,23	0,237	0,34	0,3	0,3	0,33	0,34
Nu23	0,22	0,2	0,22	0,23	0,25	0,28	0,42	0,34	0,3	0,3	0,33	0,34
Nu13	0,43	0,45	0,41	0,38	0,32	0,28	0,231	0,34	0,3	0,3	0,33	0,34
G12 (GPa)	6,9	7,5	7,6	7,4	7,2	7,2	4,7	6,6	0,115	0,000385	44	38
G23 (GPa)	4,8	5,1	5	5	5,2	5,3	3,6	6,6	0,115	0,000385	44	38
G13 (GPa)	5,3	5,5	5,5	5,4	5,5	5,8	4,7	6,6	0,115	0,000385	44	38

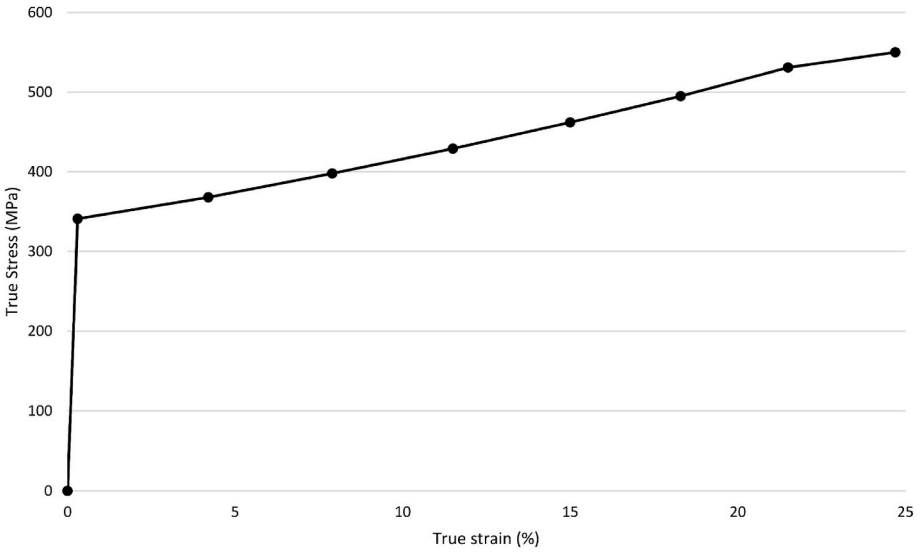

Fig. 2. True stress – true strain curve for pure titanium calculated using the values nominal yield stress (340 MPa), nominal ultimate stress (430 MPa), top value of nominal strain (28 %) and Young's modulus (102 GPa), interpolation of the nominal values to obtain the curve [14].

The strain distributions during incisal biting are illustrated in Fig. 4. As in unilateral biting, pre-bending did not affect intersegmental strains. Posterior strains (posterior customized conventional reconstruction plate percentiles 1–2.3 %, 0.75–0.8 %, 0.5–0.5 %, 0.25–0.3 %; anterior pre-bent conventional reconstruction plate percentiles 1–2.4 %, 0.75–0.8 %, 0.5–0.5 %, 0.25–0.3 %) were higher than anterior strains (anterior customized conventional reconstruction plate percentiles 1–1.4 %, 0.75–0.5 %, 0.5–0.3 %, 0.25–0.2 %; anterior pre-bent conventional reconstruction plate percentiles 1–1.5 %, 0.75–0.6 %, 0.5–0.3 %, 0.25–0.2 %). Incisal biting generally resulted in lower strains compared to unilateral biting. Nevertheless, the difference between anterior and posterior strain levels were smaller compared to unilateral biting (see Figs. 3 and 4).

3.2. Pre-bending induces maximum stresses in the plastic phase of titanium

Stress distributions within the plates before and during unilateral- and incisal biting and the peaks in von Mises stresses are shown in Fig. 5. Pre-bending caused plastic stresses (maximum of 464 MPa) that led to permanent deformation (over 341 MPa) in multiple locations. After unilateral biting, the pre-bent reconstruction plate presented a slightly wider spatially distributed stress plot with a peak stress of 447 MPa in the plastic phase. The customized reconstruction plate shows all over the plate much lower stresses (in the elastic phase) in comparison to the pre-stressed reconstruction plate. This is represented by a maximum stress value of 41 MPa in the customized plate.

In incisal biting, analogously to unilateral biting, the pre-bent plate experienced stress values in the plastic phase. The maximum stress value of the pre-bent reconstruction plate was 447 MPa. Without pre-bending, the plate showed lower stresses in the elastic phase. This observation is represented by a maximum stress of 21 MPa in the customized reconstruction plate. Generally, under incisal biting, the customized reconstruction plate was less stressed than the same plate under unilateral biting (see Fig. 5). In the pre-stressed scenarios, both biting tasks induced similar maximum stresses.

4. Discussion

Although patient-specific 3D-printed reconstruction plates are

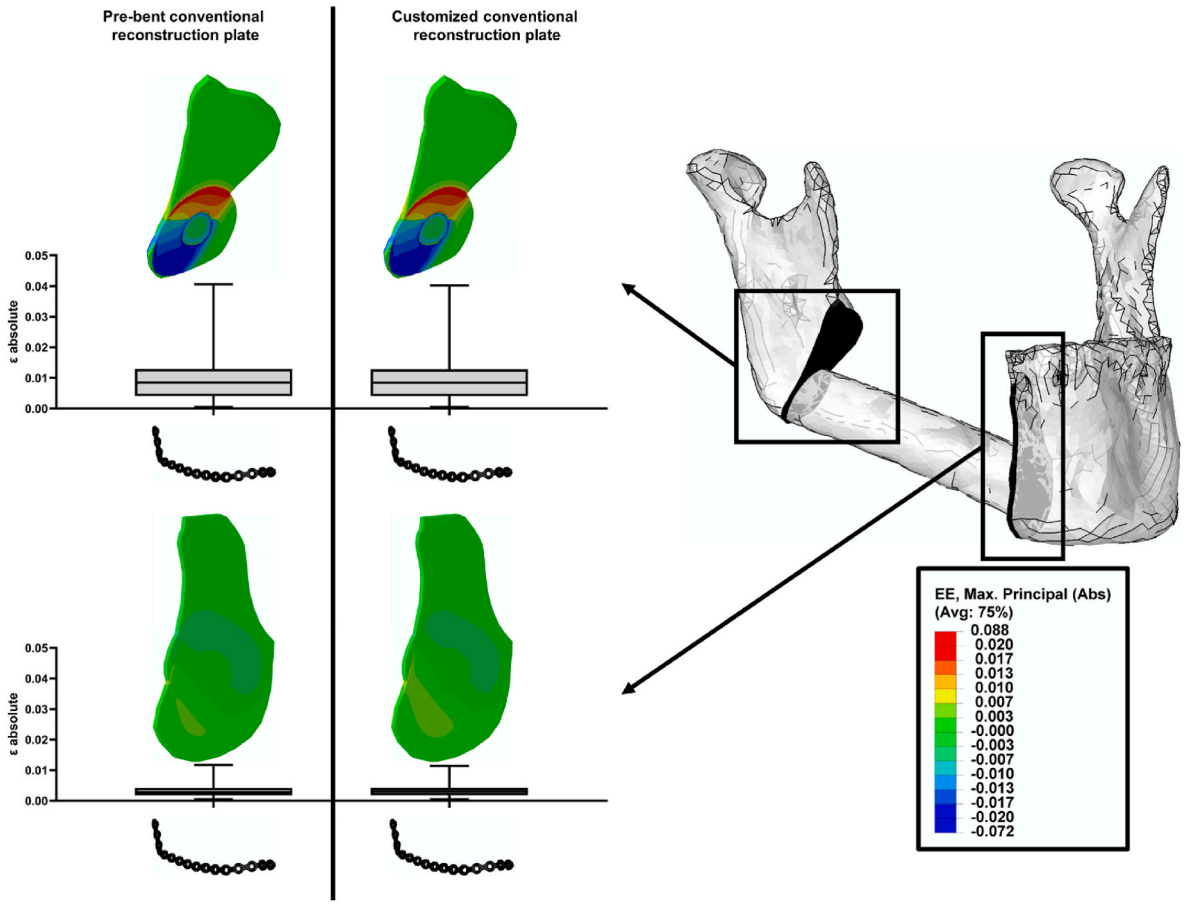

Fig. 3. Unilateral biting induced quantitative (boxplots, percentiles 0.75, 0.5, 0.25) strain distributions and contour plots of the anterior (bottom) and posterior (top) intersegmental gaps in the pre-stressed (left) and customized reconstruction plate (right) scenarios.

mostly advantageous over conventional reconstruction plates, conventional reconstruction plates present higher rates of osseous union [2,4,6]. To understand the reasons for this observation, pre-bent and customized conventional reconstruction plates have been biomechanically evaluated in the present study. The results suggest that the plate pre-bending does not alter mechanical strains within the healing region under conventional fixation. However, plate pre-bending induces plastic mechanical stresses within the titanium reconstruction plate [10].

A previous study evaluated the stresses induced by plate pre-bending in comparison to same-shaped customized plates under biting in a C-type symphysis reconstruction [10,41]. Similar to the present study, stresses in the plastic phase were reported for pre-stressed plates [10]. In contrast, customized conventional reconstruction plates induced reversible elastic stresses [10]. Thus, the use of customized conventional plates instead of pre-bent conventional plates could ensure a long-lasting plate performance. However, the previous study evaluating plate pre-bending did not investigate intersegmental strains [10]. Strain levels induced by common patient-specific plates have been investigated in other previous studies [16,17]. Within the present study, the two approaches have been combined to evaluate the influence of plate pre-bending on intersegmental strains.

For long bones, intersegmental strain levels favoring specific cell differentiation patterns have been determined [18,20,21]. The exact strain levels beneficial for bone healing in the mandible remain unclear [16,17,25,42]. However, previous studies suggest that bone formation positively correlates with the mechanical stimulus (strain) on the reconstructed mandible [16,42,43]. Similar to previous studies on the mandible, in the present study under unilateral biting, anterior mechanical strains were lower than posterior strains [16,17,26]. In patient-specific reconstruction plates, this is suspected to be causal for a significantly better healing outcome in the posterior areas [16,23].

Independent retrospective studies found better healing outcomes of conventional reconstruction plates in comparison to patient-specific reconstruction plates suspecting biomechanical causes [2,4,6]. However, in the present study, the mechanical process of plate pre-bending was shown not to alter the biomechanics in the healing regions when comparing the patient-specific customized conventional reconstruction plate and the pre-bent conventional reconstruction plate. In consequence, plate pre-bending is unlikely to be causal for the difference in the healing outcome. Additional simulations with customized conventional and common patient-specific plates have shown that intersegmental strains are twice as high under customized conventional reconstruction plate fixation compared to the common patient-specific reconstruction plate under both incisal and unilateral biting (Appendix 1). Previously, the distances of the screws to the osteotomies have been shown to determine the interfragmentary strains on long bones, particularly the screws closest to the osteotomy are limiting the interfragmentary strain [44]. Therefore, the placement of the first screw further away from the osteotomy can increase the intersegmental strain. This could partially explain the increased strain under customized conventional reconstruction plate fixation in comparison to common patient-specific reconstruction plate fixation.

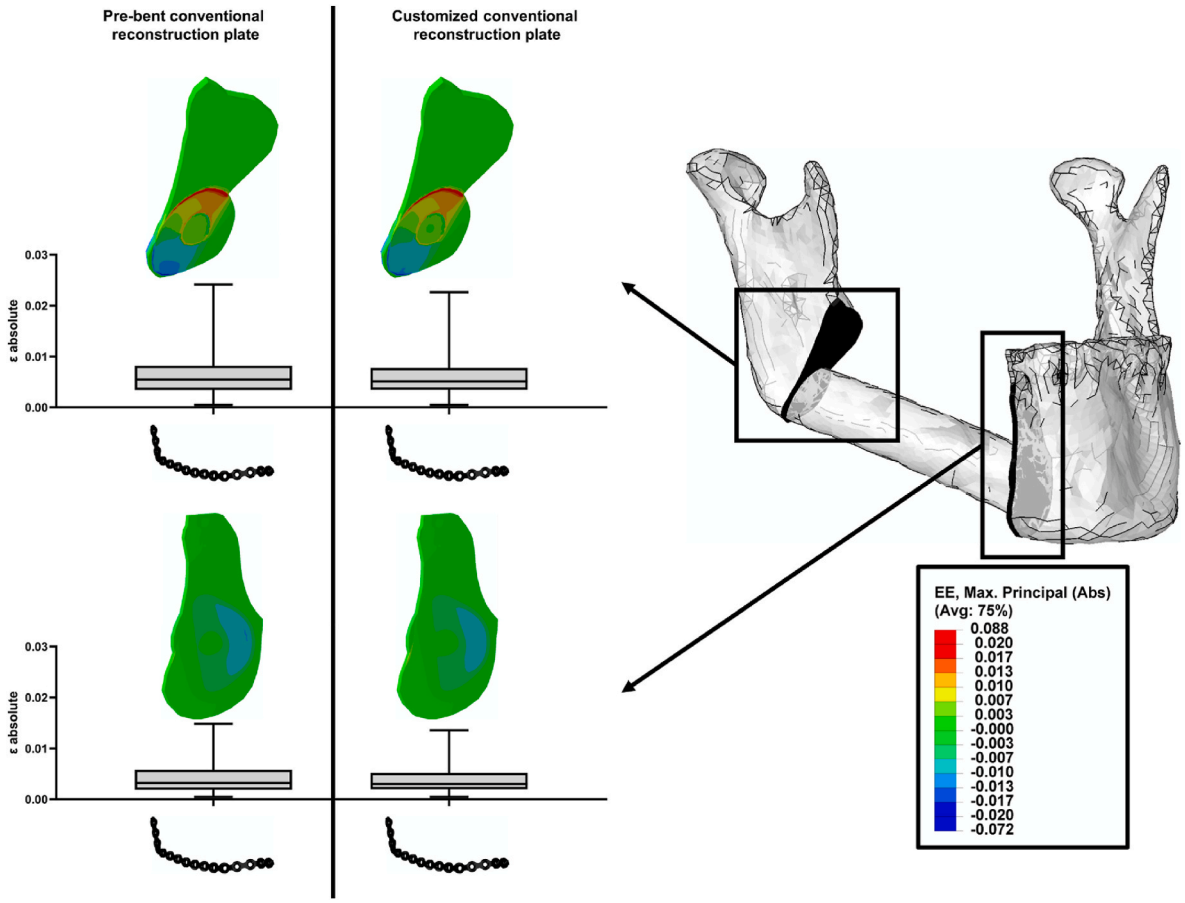

Fig. 4. Incisal biting induced quantitative (boxplots, percentiles 0.75, 0.5, 0.25) strain distributions and contour plots of the anterior (bottom) and posterior (top) intersegmental gaps in the pre-stressed (left) and customized reconstruction plate (right) scenarios.

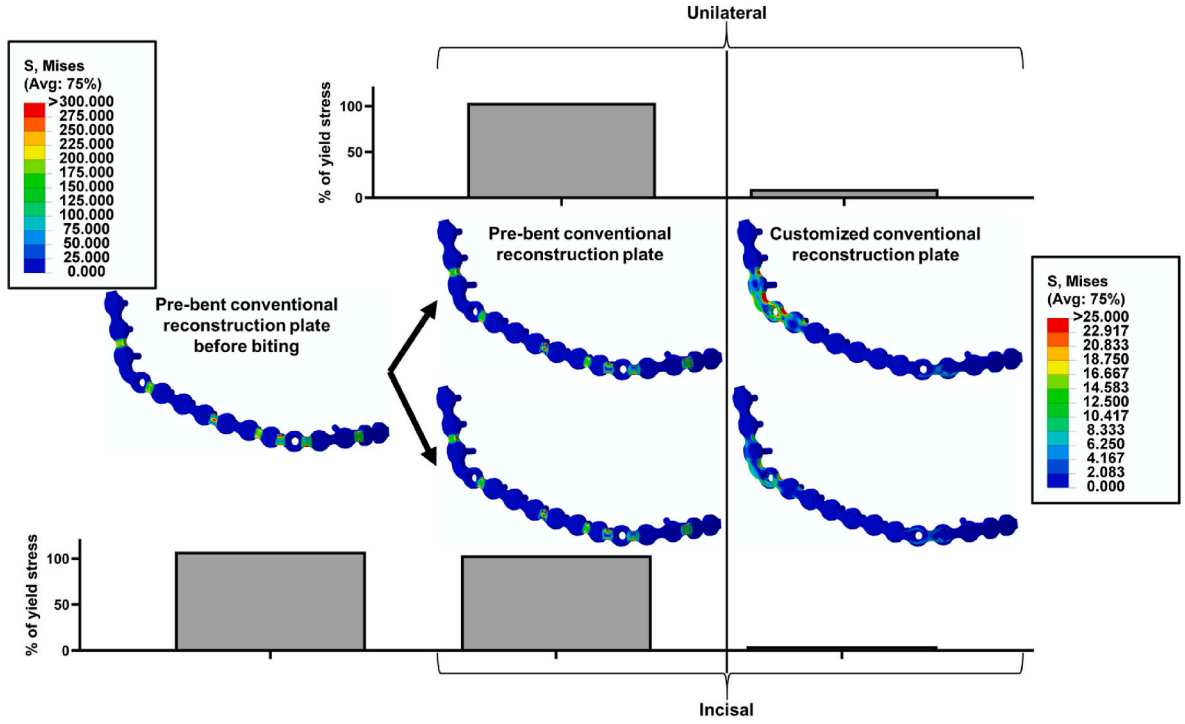

Fig. 5. Maximum (bars) von Mises stresses in % of the yield stress and von Mises stress contour plots of the pre-stressed (left) and the customized reconstruction plate (right) before and after unilateral (top) and incisal biting (bottom) with individual legends in MPa (all elements with stress values beyond the legend's top value marked in red). (For interpretation of the references to colour in this figure legend, the reader is referred to the Web version of this article.)

In the present study, material properties were simplified by applying linear elastic and linear plastic material properties. Additionally, pre-bending was simulated with kinematic constraints between the cross-sections and their midpoints, which might represent a simplification of the bending process. However, excluding the largest 0.03 % of all stress values from the analysis was intended to reduce the effect of this limitation. Only one patient was analyzed to isolate biomechanical differences between the plating groups, however, future studies should investigate different patients and clinical scenarios. Only reconstruction plates have been evaluated although conventional miniplates would be a clinical alternative [45–47]. However, since clinical studies comparing conventional reconstruction plates with patient-specific reconstruction plates are available, a comparison of a customized and a pre-bent conventional reconstruction plate was chosen to relate the biomechanical outcome to clinical data [2,4,6]. Future studies could evaluate the biomechanical and clinical influence of conventional miniplate fixation and verify the observations regarding pre-stress in a different plating configuration. The initial healing phase was evaluated in the present study and the intersegmental strains were considered positively correlated to the bone formation. The underlying mechanoregulation theories describe the effect of mechanical cues on bone regeneration [18,19]. The resulting tissue differentiation theories are mainly based on the early studies by Pauwels who proposed that tissue differentiation within a healing region was governed by mechanical stimuli [48]. He theorized that cartilage forms as a result of local hydrostatic pressure causing mesenchymal stem cells to become chondroblasts, whereas bone and fibrous tissues resulted from shear strains causing mesenchymal stem cells to differentiate into osteoblasts and fibroblasts, respectively [21, 48]. In consequence, bone healing is a multi-stage process and in the validation of the underlying mechanoregulation theory, the later stages can be modeled by coupling finite element analysis with tissue differentiation algorithms [49–51]. Nevertheless, the initial healing phase is the crucial phase for bone formation and therefore was chosen for the present study [19].

In conclusion, pre-bending causes stresses in the plastic phase which could increase the risk of material failure. However, the geometrical design of conventional reconstruction plates is likely to be causal for the increased intersegmental strains compared to common patient-specific plates. These higher intersegmental strains might be the reason for the better healing outcome of conventional plates compared to common patient-specific plates. Therefore, the design of customized conventional reconstruction plates instead of common patient-specific plates could result in a better healing outcome.

CRediT authorship contribution statement

Philipp Ruf: Writing – original draft, Visualization, Validation, Software, Methodology, Investigation, Formal analysis, Data curation, Conceptualization. **Özgür Cebeci:** Writing – review & editing, Software, Methodology, Investigation, Data curation. **Vincenzo Orassi:** Writing – review & editing, Software, Methodology. **Claudius Steffen:** Writing – review & editing, Project administration, Data curation. **Georg N. Duda:** Writing – review & editing, Resources. **Max Heiland:** Writing – review & editing, Resources, Project administration. **Sara Checa:** Writing – original draft, Supervision, Resources, Project administration, Methodology, Funding acquisition, Conceptualization. **Carsten Rendenbach:** Writing – original draft, Supervision, Project administration, Methodology, Funding acquisition, Conceptualization.

Declaration of competing interest

The authors declare the following financial interests/personal relationships which may be considered as potential competing interests: Max Heiland received speaker remuneration and research funding for other projects by Karl Leibinger Medizintechnik GmbH & Co. KG. Carsten Rendenbach received research funding for other projects by Karl Leibinger Medizintechnik GmbH & Co. KG.

Acknowledgements

The authors acknowledge the support of the European Union (EU) Horizon 2020 for the project InterLynk (grant agreement: H2020-NMBP-TR-IND-2020, project ID: 953169). This study was partially funded by the German Research Foundation (Deutsche Forschungsgemeinschaft (CH 1123/10-1 and RE 4803/1-1)). The authors acknowledge the support of Clarence Janka, design engineer with Karl Leibinger Medizintechnik GmbH & Co. KG, in the virtual deformation of the conventional plates.

Appendix

Both plates (customized conventional reconstruction plate and common patient-specific plate) were designed as patient-specific and made from the titanium alloy Ti6Al4V that is usually used for patient-specific plates [16]. The common patient-specific plate geometry was originally generated for a previous study and has been investigated in the modified model of the present study [16]. The plates presented the following geometrical differences (Appendix 1) that have been previously described *in vitro* and *in vivo* (radiographic) [4,7]:

- Conventional reconstruction plates present slimmer bridges between the screw holes in comparison to common patient-specific plates to facilitate pre-bending.
- Conventional reconstruction plates present greater distances from the first screws to the osteotomies. Screw holes in the conventional plates have defined distances to each other and subsequently screw holes are regularly located very close to the osteotomies. These screw holes cannot be used for screws. Therefore, the screws are located more distant from the osteotomy compared to patient-specific reconstructions, in which the screw holes can be placed at a defined distance to the osteotomy and are therefore usually placed closer to the osteotomy.

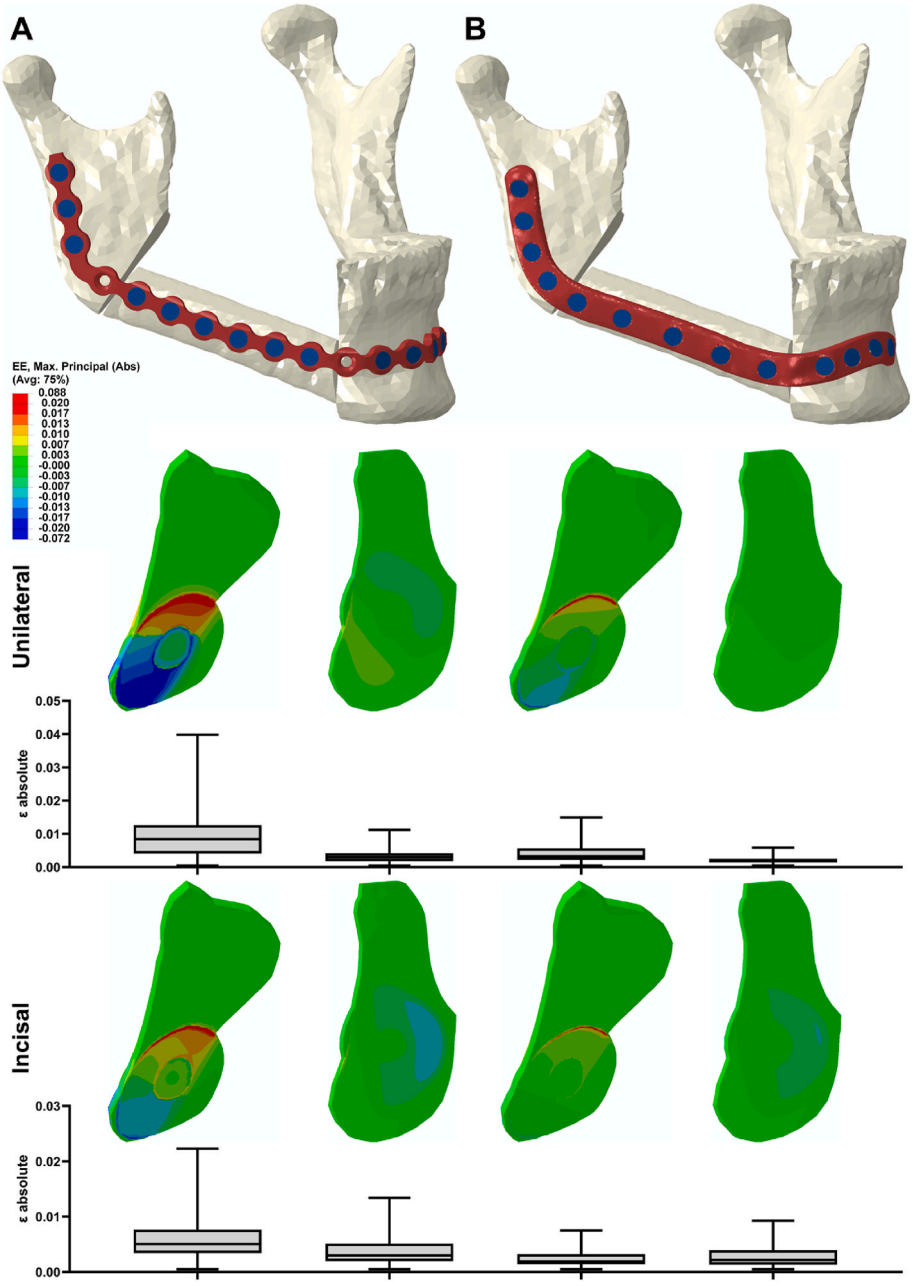

Appendix 1. Visual comparison of plate and screw configuration and variance in strains in the anterior and posterior intersegmental gap under unilateral (top) and incisal biting (bottom): (A) customized conventional reconstruction plate and (B) common patient-specific reconstruction plate both made from Ti6Al4V.

References

[1] J.S. Brown, D. Lowe, A. Kanatas, A. Schache, Mandibular reconstruction with vascularised bone flaps: a systematic review over 25 years, Br. J. Oral Maxillofac. Surg. 55 (2) (2017) 113–126.

[2] C. Rendenbach, C. Steffen, H. Hanken, K. Schluermann, A. Henningsen, B. Beck-Broichsitter, K. Kreutzer, M. Heiland, C. Precht, Complication rates and clinical outcomes of osseous free flaps: a retrospective comparison of CAD/CAM versus conventional fixation in 128 patients, Int. J. Oral Maxillofac. Surg. 48 (9) (2019) 1156–1162.

[3] N.S.J. Tang, I. Ahmadi, A. Ramakrishnan, Virtual surgical planning in fibula free flap head and neck reconstruction: a systematic review and meta-analysis, J. Plast. Reconstr. Aesthetic Surg. 72 (9) (2019) 1465–1477.

[4] M. Knitschke, S. Sonnabend, F.C. Roller, J. Pons-Kühnemann, D. Schmermund, S. Attia, P. Streckbein, H.-P. Howaldt, S. Böttger, Osseous union after mandible reconstruction with fibula free flap using manually bent plates vs. patient-specific implants: a retrospective analysis of 89 patients, Curr. Oncol. 29 (5) (2022) 3375–3392.

[5] C. Rendenbach, N. Hölterhoff, S. Hischke, K. Kreutzer, R. Smeets, A.T. Assaf, M. Heiland, J. Wikner, Free flap surgery in Europe: an interdisciplinary survey, Int. J. Oral Maxillofac. Surg. 47 (5) (2018) 676–682.

[6] M. Knitschke, M. Yonan, F.C. Roller, J. Pons-Kühnemann, S. Attia, H.-P. Howaldt, P. Streckbein, S. Böttger, Osseous union after jaw reconstruction with fibula-free flap: conventional vs. CAD/CAM patient-specific implants, Cancers 14 (23) (2022).

[7] C. Rendenbach, K. Sellenschloh, L. Gerbig, M.M. Morlock, B. Beck-Broichsitter, R. Smeets, M. Heiland, G. Huber, H. Hanken, CAD-CAM plates versus conventional fixation plates for primary mandibular reconstruction: a biomechanical in vitro analysis, J. cranio-maxillo-facial surg. Off Pub. Europ. Ass. Cranio-Maxillo-Facial Surg. 45 (11) (2017) 1878–1883.

[8] C. Steffen, A.P. Soares, T. Heintzelmann, H. Fischer, J.O. Voss, S. Nahles, J. Wuster, S. Koerdt, M. Heiland, C. Rendenbach, Impact of the adjacent bone on pseudarthrosis in mandibular reconstruction with fibula free flaps, Head Face Med. 19 (1) (2023) 43.

[9] W.C.H. Parr, T. Wang, C. Tan, M.J. Dan, W.R. Walsh, P. Morberg, Fatigue implications for bending orthopaedic plates, Injury 52 (10) (2021) 2896–2902.

[10] P. Si-Myung, L. Deukhee, L. Jung-Woo, K. Youngjun, K. Laehyun, N. Gunwoo, Stability of the permanently bent plates used in mandibular reconstructive surgery, Annu. Int. Conf. IEEE Eng. Med. Biol. Soc. (2016) 2198–2201.
[11] C. Steffen, K. Sellenschloh, M. Vollmer, M.M. Morlock, M. Heiland, G. Huber, C. Rendenbach, Biomechanical comparison of titanium miniplates versus a variety of CAD/CAM plates in mandibular reconstruction, J. Mech. Behav. Biomed. Mater. 111 (2020) 104007.
[12] KLS, Osteosynthese 2.0 - 2.7 Fraktur und Rekonstruktion Threadlock TS. https://www.klsmartin.com/mediathek/90-442-01-04_LevelOne_Fixation_Osteosynthese_2_0-2_7_Fraktur_und_Rekonstruktion_Threadlock_TS.pdf, 2023. (Accessed 28 May 2024).
[13] KLS, LevelOne fixation osteosynthese 2.0 mini. https://www.klsmartin.com/mediathek/90-443-01-04_LevelOne_Fixation_Osteosynthese_2.0_Mini.pdf, 2023. (Accessed 28 May 2024).
[14] MatWeb, Titanium grade 2, annealed. https://www.matweb.com/search/datasheet.aspx?MatGUID=49a4b764217b44ee953205822af5fbc9, 2024. (Accessed 19 June 2024).
[15] MatWeb, Titanium Ti-6Al-4V (grade 5), annealed bar. https://www.matweb.com/search/DataSheet.aspx?MatGUID=10d463eb3d3d4ff48fc57e0ad1037434, 2024. (Accessed 19 June 2024).
[16] P. Ruf, V. Orassi, H. Fischer, C. Steffen, G.N. Duda, M. Heiland, K. Kreutzer, S. Checa, C. Rendenbach, Towards mechanobiologically optimized mandible reconstruction: CAD/CAM miniplates vs. reconstruction plates for fibula free flap fixation: a finite element study, Front. Bioeng. Biotechnol. 10 (2022).
[17] P. Ruf, V. Orassi, H. Fischer, C. Steffen, K. Kreutzer, G.N. Duda, M. Heiland, S. Checa, C. Rendenbach, Biomechanical evaluation of CAD/CAM magnesium miniplates as a fixation strategy for the treatment of segmental mandibular reconstruction with a fibula free flap, Comput. Biol. Med. 168 (2024) 107817.
[18] L.E. Claes, C.A. Heigele, Magnitudes of local stress and strain along bony surfaces predict the course and type of fracture healing, J. Biomech. 32 (3) (1999) 255–266.
[19] G.N. Duda, S. Geissler, S. Checa, S. Tsitsilonis, A. Petersen, K. Schmidt-Bleek, The decisive early phase of bone regeneration, Nat. Rev. Rheumatol. (2023).
[20] L. Claes, [mechanobiology of fracture healing part 2 : relevance for internal fixation of fractures], Unfallchirurg 120 (1) (2017) 23–31.
[21] L. Claes, [Mechanobiology of fracture healing part 1 : Principles], Unfallchirurg 120 (1) (2017) 14–22.
[22] A.S. Reference, Fibula osteocutaneous flap harvest. https://surgeryreference.aofoundation.org/cmf/reconstruction/basic-technique/fibula-osteocutaneous-flap#introduction, 2013. (Accessed 28 February 2021).
[23] C. Steffen, H. Fischer, M. Sauerbrey, T. Heintzelmann, J.O. Voss, S. Koerdt, S. Checa, K. Kreutzer, M. Heiland, C. Rendenbach, Increased rate of pseudarthrosis in the anterior intersegmental gap after mandibular reconstruction with fibula free flaps: a volumetric analysis, Dentomaxillofacial Radiol. 51 (7) (2022) 20220131.
[24] S. Hashemi, M. Oda, K. Onoue, K. Basa, S.J. Rubin, O. Sakai, A. Salama, W.H. Ezzat, Determining the optimal osteotomy distance with the fibula free flap in mandibular reconstruction, Am. J. Otolaryngol. 41 (3) (2020) 102436.
[25] V. Orassi, G.N. Duda, M. Heiland, H. Fischer, C. Rendenbach, S. Checa, Biomechanical assessment of the validity of sheep as a preclinical model for testing mandibular fracture fixation devices, Front. Bioeng. Biotechnol. 9 (2021) 672176.
[26] V. Orassi, H. Fischer, G.N. Duda, M. Heiland, S. Checa, C. Rendenbach, In silico biomechanical evaluation of WE43 magnesium plates for mandibular fracture fixation, Front. Bioeng. Biotechnol. 9 (2021) 803103.
[27] H. Aftabi, K. Zaraska, A. Eghbal, S. McGregor, E. Prisman, A. Hodgson, S. Fels, Computational models and their applications in biomechanical analysis of mandibular reconstruction surgery, Comput. Biol. Med. 169 (2024) 107887.
[28] ABAQUS, Abaqus version 6.6 documentation. https://classes.engineering.wustl.edu/2009/spring/mase5513/abaqus/docs/v6.6/books/gss/default.htm?startat=ch08s02.html, 2006. (Accessed 19 June 2024).
[29] K. Kreutzer, C. Steffen, S. Nahles, S. Koerdt, M. Heiland, C. Rendenbach, B. Beck-Broichsitter, Removal of patient-specific reconstruction plates after mandible reconstruction with a fibula free flap: is the plate the problem? Int. J. Oral Maxillofac. Surg. 51 (2) (2022) 182–190.
[30] A.S. Reference, Plate and fibular osteocutaneous free flap: symphysis and skin. https://surgeryreference.aofoundation.org/cmf/reconstruction/mandible/symphysis-and-skin/plate-and-fibular-osteocutaneous-free-flap#reconstruction, 2013. (Accessed 16 March 2022).
[31] T.W. Korioth, A.G. Hannam, Deformation of the human mandible during simulated tooth clenching, J. Dent. Res. 73 (1) (1994) 56–66.
[32] T.W. Korioth, D.P. Romilly, A.G. Hannam, Three-dimensional finite element stress analysis of the dentate human mandible, Am. J. Phys. Anthropol. 88 (1) (1992) 69–96.
[33] H. Gheibollahi, E. Aliabadi, M.S. Khaghaninejad, S. Mousavi, A. Babaei, Evaluation of bite force recovery in patients with maxillofacial fracture, Journal of cranio-maxillo-facial surgery : Off Pub. Europ. Ass. Cranio-Maxillo-Facial Surg. (2021).
[34] C.L. Schwartz-Dabney, P.C. Dechow, Variations in cortical material properties throughout the human dentate mandible, Am. J. Phys. Anthropol. 120 (3) (2003) 252–277.
[35] S.T. Lovald, J.D. Wagner, B. Baack, Biomechanical optimization of bone plates used in rigid fixation of mandibular fractures, J. Oral Maxillofac. Surg. : Off. J. Am. Assoc. Oral Maxillofacial Surg. 67 (5) (2009) 973–985.
[36] J.Y. Rho, An ultrasonic method for measuring the elastic properties of human tibial cortical and cancellous bone, Ultrasonics 34 (8) (1996) 777–783.
[37] E. Lefèvre, P. Lasaygues, C. Baron, C. Payan, F. Launay, H. Follet, M. Pithioux, Analyzing the anisotropic Hooke's law for children's cortical bone, J. Mech. Behav. Biomed. Mater. 49 (2015) 370–377.
[38] É. Lakatos, L. Magyar, I. Bojtár, Material properties of the mandibular trabecular bone, J. Med. Eng. 2014 (2014) 470539.
[39] P.L. Leong, E.F. Morgan, Measurement of fracture callus material properties via nanoindentation, Acta Biomater. 4 (5) (2008) 1569–1575.
[40] H.J. Motulsky, R.E. Brown, Detecting outliers when fitting data with nonlinear regression - a new method based on robust nonlinear regression and the false discovery rate, BMC Bioinf. 7 (2006) 123.
[41] J.B. Boyd, P.J. Gullane, L.E. Rotstein, D.H. Brown, J.C. Irish, Classification of mandibular defects, Plast. Reconstr. Surg. 92 (7) (1993) 1266–1275.
[42] S.-M. Park, J.-W. Lee, G. Noh, Which plate results in better stability after segmental mandibular resection and fibula free flap reconstruction? Biomechanical analysis, Oral Surg. Oral Med. Oral Pathol. Oral Radiol. 126 (5) (2018) 380–389.
[43] N. Yoda, K. Zheng, J. Chen, Z. Liao, S. Koyama, C. Peck, M. Swain, K. Sasaki, Q. Li, Biomechanical analysis of bone remodeling following mandibular reconstruction using fibula free flap, Med. Eng. Phys. 56 (2018) 1–8.
[44] Z. Li, S. Pollard, G. Smith, S. Deshmukh, Z. Ding, Biomechanical analysis of combi-hole locking compression plate during fracture healing: a numerical study of screw configuration, Proc. Inst. Mech. Eng. H 238 (3) (2024) 313–323.
[45] A.B. Robey, M.L. Spann, T.M. McAuliff, J.L. Meza, R.R. Hollins, P.J. Johnson, Comparison of miniplates and reconstruction plates in fibular flap reconstruction of the mandible, Plast. Reconstr. Surg. 122 (6) (2008) 1733–1738.
[46] S.C. Fontana, R.B. Smith, N. Nazir, B.T. Andrews, Biomechanical assessment of fixation methods for segmental mandible reconstruction with fibula in the polyurethane model, Microsurgery 36 (4) (2016) 330–333.
[47] E. Zavattero, M. Fasolis, P. Garzino-Demo, S. Berrone, G.A. Ramieri, Evaluation of plate-related complications and efficacy in fibula free flap mandibular reconstruction, J. Craniofac. Surg. 25 (2) (2014) 397–399.
[48] F. Pauwels, Eine neue Theorie über den Einfluß mechanischer Reize auf die Differenzierung der Stützgewebe, Z. Anat. Entwicklungsgeschichte 121 (6) (1960) 478–515.
[49] E. Borgiani, G.N. Duda, S. Checa, Multiscale modeling of bone healing: toward a systems biology approach, Front. Physiol. 8 (2017) 287.
[50] A.-M. Pobloth, S. Checa, H. Razi, A. Petersen, J.C. Weaver, K. Schmidt-Bleek, M. Windolf, A.Á. Tatai, C.P. Roth, K.-D. Schaser, G.N. Duda, P. Schwabe, Mechanobiologically optimized 3D titanium-mesh scaffolds enhance bone regeneration in critical segmental defects in sheep, Sci. Transl. Med. 10 (423) (2018).
[51] M. Jaber, P.S.P. Poh, G.N. Duda, S. Checa, PCL strut-like scaffolds appear superior to gyroid in terms of bone regeneration within a long bone large defect: an in silico study, Front. Bioeng. Biotechnol. 10 (2022).